PTEP

Prog. Theor. Exp. Phys. **2014**, 06B101 (13 pages)
DOI: 10.1093/ptep/ptu073

CMB Cosmology

Introduction to temperature anisotropies of Cosmic Microwave Background radiation

Naoshi Sugiyama[1,2,3,*]

[1]*Department of Physics, Nagoya University, Nagoya, 464-8602, Japan*
[2]*Kobayashi Maskawa Institute for the Origin of Particles and the Universe, Nagoya University, Nagoya, Japan*
[3]*Kavli IPMU, University of Tokyo, Japan*
[*]E-mail: naoshi@nagoha-u.jp

Received April 7, 2014; Revised April 28, 2014; Accepted April 30, 2014; Published June 11, 2014

Since its serendipitous discovery, Cosmic Microwave Background (CMB) radiation has been recognized as the most important probe of Big Bang cosmology. This review focuses on temperature anisotropies of CMB which make it possible to establish precision cosmology. Following a brief history of CMB research, the physical processes working on the evolution of CMB anisotropies are discussed, including gravitational redshift, acoustic oscillations, and diffusion dumping. Accordingly, dependencies of the angular power spectrum on various cosmological parameters, such as the baryon density, the matter density, space curvature of the universe, and so on, are examined and intuitive explanations of these dependencies are given.

Subject Index E56, E60, E63, E65

1. Introduction: A brief history of research on CMB

Since its serendipitous discovery in 1965 by Penzias and Wilson [1], Cosmic Microwave Background (CMB) radiation, which was first predicted by Alpher and Herman in 1948 [2] as radiation at 5 K at the present time, has become one of the most important observational probes of Big Bang cosmology. CMB is recognized as a fossil of the early universe because it directly brings information from the epoch of recombination, which is 370, 000 years after the beginning of the universe. The almost perfect blackbody shape of the energy spectrum could only be realized by the thermal equilibrium between photons, electrons, and protons in the early universe and is interpreted as evidence of the Big Bang. Its isotropic nature proves a homogeneous and isotropic universe, i.e., the Friedmann universe. CMB also brings us information from beyond the horizon scale at the recombination epoch. And it turns out that there are correlated signals beyond the horizon in the angular power spectrum of CMB which can be interpreted as partial evidence for the existence of inflation in the very early universe.

Soon after the discovery of CMB, deviations from the blackbody shape and the isotropy, which are referred to as spectral distortion and anisotropies, respectively, became the next targets for both theorists and observers. Individual physical processes to generate anisotropies, such as gravitational redshift and diffusion damping, were proposed by Sachs and Wolfe in 1967 [3] and Silk in 1968 [4], respectively. A thorough treatment of the evolution of density perturbations was given by Peebles and Yu in 1970 [5], in which the acoustic oscillations of the photon–baryon fluid are discussed.

In the meantime, intensive studies of the thermal history and structure formation of the universe and their consequences on CMB have been carried out by Sunyaev and Zeldovich [6–9] behind the Iron Curtain, following the tradition of studying perturbations in the expanding universe in a general relativistic manner which started with Lifshitz and Khalatnikov in 1964 [10]. In the former Soviet Union, Sakharov also discussed the (acoustic) oscillations of small density fluctuations in the expanding universe for the first time in 1965 (an English translation was published in 1966 [11]) while he mostly concentrated on structure formation in the universe. Accordingly, the acoustic oscillations of CMB are sometimes referred to as the Sakharov oscillations.

Since these theoretical predictions were far beyond the level of being able to be observed by any realistic experiments in those days, there was not much important work on CMB in the mid and late 1970s. It should be noted, however, that the COBE satellite was proposed in 1974 to NASA, and was one of the most important steps for CMB research, although one had to wait until 1989 for the launch for multiple reasons.

In 1981, Wilson and Silk [12] provided detailed numerical calculations of density and temperature perturbations. They treated CMB anisotropies by employing multipole expansion, taking into account the anisotropy of Thomson scattering, and derived the Boltzmann hierarchy for the CMB photon phase-space distributions. Wilson [13] extended this work for the case of non-flat geometry. Vittorio and Silk [14] and Bond and Efstathiou [15] (both in 1984) estimated CMB anisotropies for the first time in a universe dominated by non-baryonic cold dark matter. In one of the series of papers by Bond and Efstathiou, Ref. [16], they proposed the angular power spectrum in the multipole component as an observational quantity, which is widely used now. Before that, most of the authors instead employed the angular correlation function.

In the 1980s, attempts to re-write the formula of perturbations in a gauge-invariant manner were made [17,18]. With the gauge-invariant formula, the physical meaning of each perturbation variable becomes clear. Based on the gauge-invariant formula, the evolution of density and temperature fluctuations was calculated and predictions for observations were given [19,20].

The first clear detection of CMB temperature anisotropies was the dipole anisotropy [21–23]. This dipole anisotropy was, however, able to be understood as a Doppler effect caused by the peculiar motion of the solar system with respect to the CMB rest frame. Efforts to detect smaller-scale anisotropies which have the same origin in density fluctuations were, however, in vain for two decades because of experimental difficulties such as the requirement of high sensitivity, foreground emissions (which include extragalactic discrete point sources), emissions from the Galaxy such as synchrotron emission, free–free emission, dust emission, and atmospheric emission.

Finally, the COBE satellite, which was launched in 1989, made the biggest observational breakthrough for CMB science. COBE gave a stringent constraint on the spectral distortion [24–26] as well as a precise measurement of blackbody temperature. It is no doubt that the biggest achievement of COBE is, however, the discovery of temperature anisotropies in the CMB sky [27], since these tiny wrinkles on the order of 10^{-5} were believed to be the origin of structures in the universe. As a result, two COBE team members, John Mather and George Smoot, were awarded the Nobel prize in physics in 2006.

After COBE's discovery, intensive theoretical work was carried out to understand the nature of CMB temperature anisotropies. From this work, it became more and more clear that a precise measurement of CMB temperature anisotropies with much better angular resolution and higher sensitivity than COBE would lead to a new era of cosmology (see, e.g., Ref. [28]). Accordingly, three intermediate-scale satellite missions were proposed to NASA and two satellite missions from France

and Italy were proposed to ESA. From the three, NASA selected the MAP mission which was mostly driven by former COBE team members. ESA forced two missions to merge and renamed it the Planck mission in honor of the famous German physicist. The MAP satellite was launched in 2001 and the first results were announced in 2003 [29,30]. Just before the announcement, the mission was renamed to WMAP to commemorate the late Professor David Wilkinson. WMAP was actively operated for nine years and is now derelict. The Planck satellite was finally launched in 2009 together with the Herschel Space Observatory after several years' delay. With more channels at higher frequencies and much better angular resolutions and sensitivities than WMAP, Planck successfully obtained an all-sky CMB map and the operation stopped in 2013. The Planck team submitted a series of papers about the first cosmology results in 2013 with the first year's data [31,32], and is currently busy analyzing the rest of the data, especially the polarization of the CMB.

In this paper, we focus on temperature anisotropies of the CMB and summarize each physical process working in the evolution of CMB anisotropies in Sect. 2. Section 3 is devoted to explaining how the cosmological parameters are determined with the angular power spectrum of temperature anisotropies. Finally, future prospects for CMB study are discussed in Sect. 4.

2. Physical Processes

Deviations from the homogeneous and isotropic universe originate from tiny curvature fluctuations generated at the epoch of inflation. Because of their quantum origin in near de Sitter space, curvature fluctuations are expected to have little scale dependence. From the almost scale-free fluctuations, structures of the universe such as galaxies, clusters of galaxies, and large-scale structure, as well as CMB temperature fluctuations, are formed. Therefore, any specific structures in CMB temperature anisotropies are generated through physical processes working on the CMB in the expanding universe. Here we can separate temperature fluctuations of the CMB into three parts based on individual physical processes as follows.

2.1. The Sachs–Wolfe effect

The first process is gravitational red and/or blue shifts, which were pointed out by Sachs and Wolfe in 1967 [3]. The so-called Sachs–Wolfe effect is a simple redshift of CMB photons due to the density fluctuations at the last scattering surface (LSS). Here, LSS is the place where observed CMB photons were scattered by electrons the last time, which happened at the epoch of recombination when the universe was 3000 K and the redshift was 1100. If there is a higher-density region than the average at LSS, photons from this location have to climb up the potential well and are gravitationally redshifted. It is known that the amount of redshift in the case of adiabatic initial conditions is $\Psi/3$, where Ψ is the gravitational potential. On the contrary, it becomes 2Ψ for isocurvature initial conditions (see, e.g., Refs. [33,34]).

On the super-horizon scale, curvature and gravitational potential perturbations are frozen and keep their initial values as generated in the epoch of inflation. Once the perturbations enter the horizon, curvature and gravitational potential perturbations are damped away in the radiation-dominated epoch, since density perturbations of radiation cannot grow in the sub-horizon scale, although they are preserved in the matter-dominated epoch. Accordingly, the Sachs–Wolfe effect suffers damping on the scales below the horizon of the matter–radiation equality epoch, which is relatively close to the recombination epoch. Moreover, since the acoustic oscillations discussed in the next subsection provide dominant contributions in temperature anisotropies on the scales below the horizon at the recombination epoch, one can only see the Sachs–Wolfe effect as a dominant contribution in CMB

anisotropies on the super-horizon scale at LSS. The horizon scale is defined as $d_{\rm H} = a\int {\rm d}t/a$, where $a \equiv 1/(1+z)$ is a scale factor. Accordingly, the comoving horizon scale in the matter-dominated epoch can be written in terms of cosmological parameters as

$$d_{\rm H}^{\rm c} \equiv (1+z)d_{\rm H} = \frac{2c}{H_0\sqrt{\Omega_{\rm M}}}(1+z)^{-1/2}, \tag{1}$$

where H_0 and $\Omega_{\rm M}$ are the Hubble constant and the matter density parameter at present. Therefore, horizon scales at recombination $1+z_{\rm rec} \simeq 1100$ and at present are

$$d_{\rm H}^{\rm c}(t_{\rm rec}) = 180\left(\Omega_{\rm M}h^2\right)^{-1/2}\ {\rm Mpc}, \tag{2}$$

and

$$d_{\rm H}^{\rm c}(t_0) = 6000\left(\Omega_{\rm M}h^2\right)^{-1/2}\ {\rm Mpc}, \tag{3}$$

respectively, in the case of the matter-dominated universe. It should be noted that in the case of the standard flat Λ cold dark matter model (CDM), the horizon size at present is 14 Gpc with $\Omega_{\rm M} = 0.3$ and $h = 0.7$, while Eq. (3) gives 16 Gpc, which is 10% larger.

From above equations, one can estimate an angular size of the horizon scale at recombination as

$$\theta_{\rm H} = d_{\rm H}^{\rm c}(t_{\rm rec})/d_{\rm H}^{\rm c}(t_0) = 0.030\,[{\rm radian}] = 1.7\,[{\rm degree}]. \tag{4}$$

Therefore, the Sachs–Wolfe effect provides a dominant contribution on scales larger than 2°.

If there is any difference of gravitational potential energy between when photons get into and get out of the structure, the difference of energy generates redshift or blueshift on CMB photons. If the former is larger (smaller) than the latter, photons obtain (lose) the energy and are blueshifted (redshifted). Since the overall effect is obtained by integrating the variation of gravitational potential over the line of sight, this effect is referred as the Integrated Sachs–Wolfe (ISW) effect [3,35]. Note that the same physical effect caused by non-linear structure formation was first pointed out by Ress and Sciama in 1968 [36] and is often referred to as the Ress–Sciama effect.

In the case of linear perturbations during the matter-dominated or radiation-dominated eras, it is known that the gravitational potential of the structure stays constant and accordingly there is no ISW effect. The ISW effect arises at the transient epochs from radiation domination to matter domination, or from matter domination to dark energy domination. The former is called early ISW and the latter late ISW, since the transitions take place at $z = 24000\Omega_{\rm M}h^2$, where h is the non-dimensional Hubble constant normalized to $100\,{\rm km\,s^{-1}\,Mpc^{-1}}$, and at $z = (\Omega_\Lambda/\Omega_{\rm M})^{1/3} - 1$, where Ω_Λ is the density parameter of dark energy. Each effect provides a dominant contribution on the comoving horizon scale at the transition epoch in the CMB sky. Accordingly, corresponding angular scales are roughly a degree scale and a few tens of degrees scale for the early and the late ISW effects, respectively.

2.2. Acoustic oscillations

Since photons, protons, and electrons are coupled through Compton and Coulomb interactions before recombination, they can be treated as a mixed compressive fluid. It is known that the density fluctuations in a compressive fluid are acoustic waves. Therefore, perturbations of the mixed fluid start to oscillate once they cross the sound horizon. Here the sound horizon is defined as

$$d_{\rm s} \equiv a\int \frac{c_{\rm s}{\rm d}t}{a}, \tag{5}$$

where $c_{\rm s}$ is the sound speed. In the case of the photon–baryon mixed fluid, the sound speed can be written as

$$c_{\rm s}^2 \equiv \frac{\delta p}{\delta\rho} = \frac{\delta p_\gamma}{\delta(\rho_\gamma+\rho_{\rm B})} = \frac{\dot{p}_\gamma}{\dot{\rho}_\gamma+\dot{\rho}_{\rm B}} = \frac{\frac{4}{3}c^2\rho_\gamma}{4\rho_\gamma+3\rho_{\rm B}} = \frac{c^2}{3}\frac{1}{1+3\rho_{\rm B}/4\rho_\gamma}, \tag{6}$$

where p and ρ are pressure and density, respectively, the overdot is a time derivative, and suffices γ and B represent photon and baryon components, respectively.

Once perturbations enter the sound horizon, they start to oscillate as acoustic waves which can be described as $\sim C_{\rm adi}\cos kd_{\rm s}^{\rm c} + C_{\rm iso}\sin kd_{\rm s}^{\rm c}$, where $C_{\rm adi}$ and $C_{\rm iso}$ are constant factors corresponding to adiabatic and isocurvature initial conditions, respectively, and k and $d_{\rm s}^{\rm c} \equiv d_{\rm s}/a$ are the comoving wave number and the comoving sound horizon, respectively [33].

In CMB temperature anisotropies, one can only find acoustic oscillations within the angular scale corresponding to the sound horizon size at LSS, which can be roughly obtained as follows. The comoving sound horizon is approximately written by the use of the comoving horizon as $d_{\rm s}^{\rm c} \simeq (c_{\rm s}/c)d_{\rm H}^{\rm c}$, which corresponds to the angular scale

$$\theta_{\rm s} = d_{\rm s}^{\rm c}(t_{\rm rec})/d_{\rm H}^{\rm c}(t_0) \simeq (c_{\rm s}/c)\,(1+z_{\rm rec})^{-1/2} = 0.014\,[\text{radian}] = 0.80\,[\text{degree}]. \tag{7}$$

At LSS, CMB photons with acoustic modes also suffer gravitational redshift/blueshift to escape from gravitational wells. Moreover, decay of gravitational potential turns out to boost the oscillations due to resonance (see, e.g., Ref. [28]).

2.3. *Diffusion damping*

On small scales, density fluctuations of photons are damped away due to diffusion. This was first pointed out by Silk in 1968 [4], and is often called Silk damping. The diffusion scale can be calculated by employing the random walk process as follows. The number of scatterings of photons by electrons per unit time is $cn_{\rm e}\sigma_{\rm T}$, where $n_{\rm e}$ and $\sigma_{\rm T}$ are the number density of electrons and the cross section of Thomson scattering, respectively. Accordingly, the mean free path of a photon becomes $\lambda_{\rm f} = 1/n_{\rm e}\sigma_{\rm T}$. The diffusion scale due to the random walk can be written as $\lambda_{\rm d} = \sqrt{N}\lambda_{\rm f}$, where N is the number of scatterings during the age of the universe. Since the travel distance of a photon $N\lambda_{\rm f}$ is as long as the horizon size of the universe, which is $2c/H$ in the matter-dominated epoch, N is obtained by the relation $N\lambda_{\rm f} = 2c/H$, which leads to $\lambda_{\rm d} = \sqrt{N}\lambda_{\rm f} = \sqrt{2c\lambda_{\rm f}/H}$. Accordingly, the comoving diffusion scale can be written as

$$\lambda_{\rm d}^{\rm c} = (1+z)\lambda_{\rm d} = 1.62\times 10^4 \left(\Omega_{\rm M}h^2\right)^{-1/4}\left(\Omega_{\rm B}h^2\right)^{-1/2}(1+z)^{-5/4}\ \text{Mpc} \tag{8}$$

in the matter-dominated era. It should be noted that the comoving diffusion scale, below which CMB temperature fluctuations are erased, becomes larger as the universe expands. At the epoch of recombination, $1+z_{\rm rec} = 1100$,

$$\lambda_{\rm d}^{\rm c}(t_{\rm rec}) = 2.55\left(\Omega_{\rm M}h^2\right)^{-1/4}\left(\Omega_{\rm B}h^2\right)^{-1/2}\ \text{Mpc}, \tag{9}$$

which corresponds to the angular scale

$$\begin{aligned}\theta_{\rm d} = \lambda_{\rm d}^{\rm c}(t_{\rm rec})/d_{\rm H}^{\rm c}(t_0) &= 1.9\times 10^{-3}\left(\frac{\Omega_{\rm M}h^2}{0.15}\right)^{1/4}\left(\frac{\Omega_{\rm B}h^2}{0.02}\right)^{-1/2}\ [\text{radian}]\\ &= 6.4\left(\frac{\Omega_{\rm M}h^2}{0.15}\right)^{1/4}\left(\frac{\Omega_{\rm B}h^2}{0.02}\right)^{-1/2}\ [\text{arcmin}].\end{aligned} \tag{10}$$

2.4. *Angular power spectrum*

In order to compare theoretical predictions of temperature anisotropies with observational data, it is convenient to define the angular power spectrum. One can expand temperature anisotropies in terms

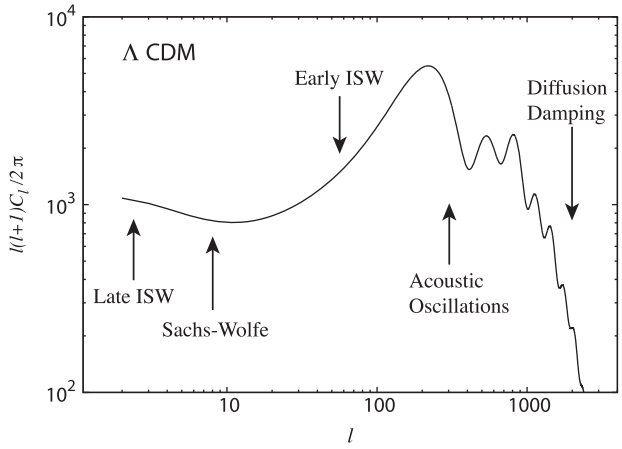

Fig. 1. The CMB angular power spectrum of the standard flat Λ CDM. Here we adopt $\Omega_\Lambda = 0.7$, $\Omega_M = 0.3$, $\Omega_B = 0.05$, $\Omega_K = 1 - \Omega_\Lambda - \Omega_M = 0$, $h = 0.7$, and $n_s = 1.0$. The normalization is arbitrary. Physical processes which provide dominant contributions on different scales are quoted.

of multipole components as $\Delta T/T \equiv \sum_{\ell=1}^{\infty} \sum_{m=-\ell}^{\ell} a_{\ell m} Y_{\ell m}$. The angular power spectrum C_ℓ is defined by the ensemble average of the square of the coefficient $a_{\ell m}$ as

$$< a_{\ell m} a^*_{\ell' m'} > \equiv C_\ell \delta_{\ell\ell'} \delta_{mm'}. \tag{11}$$

Accordingly, the ensemble average of square temperature fluctuations is written as

$$< |\Delta T/T|^2 > = \sum_{\ell\ell' mm'} < a_{\ell m} a^*_{\ell' m'} > \int \mathrm{d}\cos\theta \int \mathrm{d}\phi Y_{\ell m}(\theta, \phi) Y^*_{\ell m}(\theta, \phi) = \sum_{\ell}^{\infty} \frac{2\ell + 1}{4\pi} C_\ell. \tag{12}$$

Note here a corresponding angular scale θ for a given ℓ is $\theta\,[\mathrm{degree}] = 180/\ell$. From Eq. (12), the amplitude of temperature fluctuations in logarithmic space can be described as $\ell(2\ell + 1)C_\ell/4\pi$.

The angular power spectrum of the standard Λ CDM is shown in Fig. 1. Here, instead of $\ell(2\ell + 1)C_\ell/4\pi$, we plot $\ell(\ell + 1)C_\ell/2\pi$ since the analytic expression of the pure Sachs–Wolfe effect leads to $\ell(\ell + 1)C_\ell =$ constant for the scale-free (Harrison–Zel'dovich) initial conditions [37].

It is found that the Sachs–Wolfe effect provides a dominant contribution on large scales (small ℓs) shown as a plateau since the horizon scale at LSS [see Eq. (4)] corresponds to $\ell = 180/\theta_H = 110$. It is also seen that the late ISW effect at very large scales causes an additional enhancement of the power spectrum. At intermediate scales, acoustic oscillations are significant together with the early ISW effect near the first peak, while the diffusion damping is shown on small scales. The locations of the first peak of the acoustic oscillations and the diffusion scale are matched well with the values analytically estimated as $\ell = 180/\theta_s = 230$ [see Eq. (7)] and $\ell = 180/\theta_d = 1700$ [see Eq. (10)]. Perhaps the matching of the first peak location may be a coincidence since it turns out that $\ell \sim 300$ for the precise values of c_s and d^c_H for the standard Λ CDM. This discrepancy can be explained by a phase shift (see, e.g., Sect. 6.5 of Ref. [38]).

3. Cosmological parameter dependencies

Let us summarize the dependencies on the CMB temperature spectrum of various cosmological parameters. Current observations such as WMAP and PLANCK are so precise that these parameters can be determined typically to a percent level.

3.1. Baryon density

First, we show the dependence on the baryon density $\rho_{\rm B} \propto \Omega_{\rm B}h^2$. As is shown in Eq. (6), the sound velocity is a function of the baryon density. The larger the baryon density, the smaller the sound velocity becomes. Since the pressure of acoustic oscillations is controlled by the sound velocity, we expect larger amplitudes of acoustic peaks for a lower value of the sound velocity or a higher value of the baryon density. However, the situation is a bit more complicated. Let us employ an analogy of balls and a spring system in a gravitational well [28]. The ball was pulled and set at the initial location, and the ball starts to oscillate once the perturbations enter the sound horizon. The first compression and rarefaction correspond to the first and second peaks in the angular power spectrum, respectively. Since the initial location of perturbations is fixed regardless of the value of the baryon density or the sound velocity, the amplitudes of rarefactions or the even peaks stay at the same value while the amplitudes of compressions or odd peaks are enhanced when the baryon density $\Omega_{\rm B}h^2$ increases. If there were no diffusion, odd peaks would always be higher than even peaks and the differences in height would become larger as baryon density increases. This tendency is shown in Fig. 2, where the diffusion modifies the amplitudes of higher acoustic peaks.

The diffusion damping scale also depends on the baryon density, as is seen in Eq. (10), while it has weak dependence on the matter density too. As one increases the baryon density $\Omega_{\rm B}h^2$, the diffusion scale becomes smaller and the cutoff scale in the angular power spectrum moves in the direction of larger ℓ.

3.2. Matter density

Let us now investigate the dependence on the matter density $\Omega_{\rm M}h^2$. As shown in Eqs. (4) and (7), the matter density dependence is canceled for the angular scales of the horizon and the sound horizon, while we ignore a weak dependence of the horizon scale on dark energy in these equations. The most significant contribution of the matter density on the angular power spectrum comes from the transition from the radiation-dominated era to the matter-dominated era, since gravitational potential decays in this transition period and accordingly the temperature fluctuations are boosted. Moreover, if the transition epoch is close enough to the recombination epoch, the early ISW effect provides a large contribution to the power spectrum. Since the matter–radiation equality epoch is described as $1 + z_{\rm eq} = 24000\Omega_{\rm M}h^2$, the boost and the ISW effect are more prominent on larger scales (smaller ℓ)

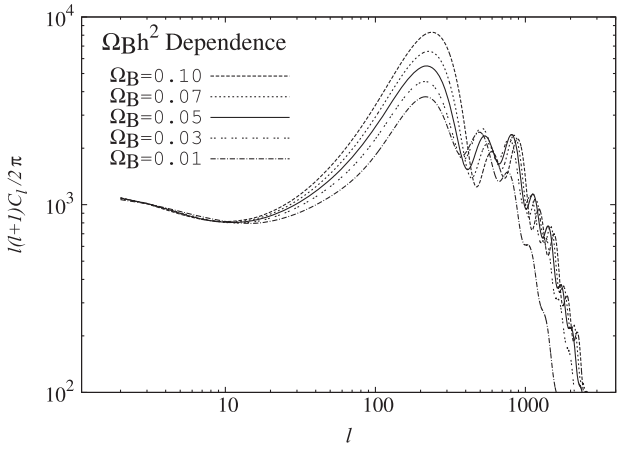

Fig. 2. Baryon density dependence on the CMB angular power spectrum. We fix the matter density $\Omega_{\rm M}h^2$ and change the baryon density $\Omega_{\rm B}h^2$ by shifting $\Omega_{\rm B}$.

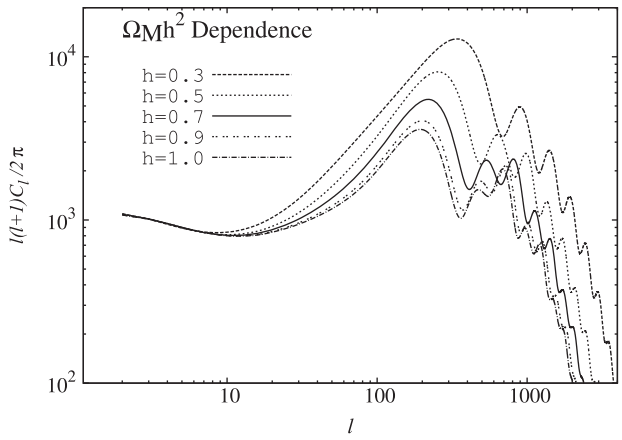

Fig. 3. Matter density dependence on the CMB angular power spectrum. We fix the baryon density $\Omega_B h^2$ and change the matter density $\Omega_M h^2$ by shifting h to keep the geometry of the universe (or the angular diameter distance to LSS).

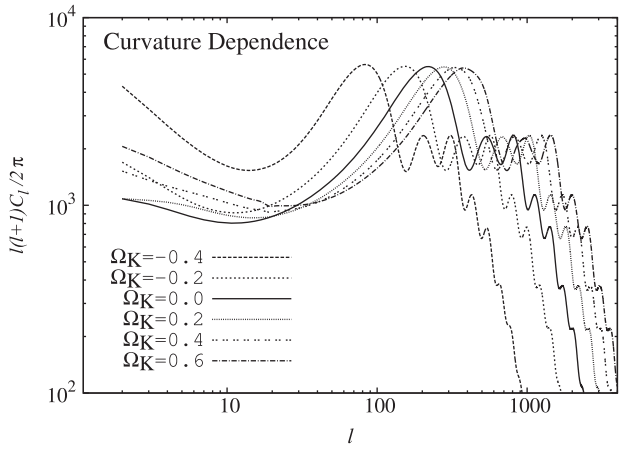

Fig. 4. Space curvature dependence on the CMB angular power spectrum. Here, Ω_K is defined as $\Omega_K \equiv 1 - \Omega_\Lambda - \Omega_M$. Accordingly, negative (positive) Ω_K corresponds to positively (negatively) curved space. In order to keep the matter density $\Omega_M h^2$, we only change Ω_Λ to shift the curvature.

for a smaller value of the matter density. As shown in Fig. 3, the amplitude of the angular power spectrum at the scale corresponding to the horizon at LSS, i.e. $\ell \sim 110$, becomes larger along with the amplitude of the first acoustic peak, as the baryon density $\Omega_M h^2$ becomes smaller.

3.3. Space curvature

The angular power spectrum also depends on the space curvature of the universe due to the modification of an apparent angular size. Compared with the case of flat space, the apparent angular size of the same object at LSS becomes larger (smaller) for positively (negatively) curved space. Accordingly, the acoustic peaks and the diffusion damping scale shifts to smaller (larger) ℓ, respectively, as shown in Fig. 4.

3.4. Initial condition

Generally speaking, there are two independent modes in density perturbations corresponding to the initial conditions. The adiabatic mode is the one generated by the curvature perturbations, while the isocurvature mode is driven by the entropy perturbations (see, e.g., Ref. [33]). In the case of

the isocurvature initial condition, density perturbations of photons and of other components, i.e., CDM, baryons, or neutrinos, are balanced and the total curvature perturbations vanish. For example, CMD isocurvature conditions satisfy $\delta\rho_\gamma + \delta\rho_{\rm CDM} = 0$ while $S_{{\rm CDM}\gamma} \equiv \delta(n_{\rm CDM}/s)/(n_{\rm CDM}/s) \neq 0$, where $n_{\rm CDM}$ and s are the number density of CDM and the entropy density of photons, respectively.

Until now, we have only considered adiabatic initial conditions. If we employ isocurvature initial conditions, however, the shape of the angular power spectrum becomes quite different. This is due to the fact that adiabatic and isocurvature modes of acoustic oscillations can be written as $\sin kd_{\rm s}^{\rm c}$ and $\cos kd_{\rm s}^{\rm c}$, respectively. Accordingly, there is a difference of $\pi/2$ in the phase of oscillations. As shown in Fig. 5, the locations of the peaks for isocurvature modes correspond to troughs for adiabatic modes, and vice versa. Here we employ CDM isocurvature initial conditions.

3.5. *Optical depth*

It is known that the intergalactic medium (IGM), which once became neutral through the recombination process at 370,000 years after the beginning of the universe, was reionized by UV radiation from first stars or active galactic nuclei. From recent surveys of quasi-stellar objects by SDSS, it has become clear that the reionization process was completed by $z \sim 6$ (see, e.g., Ref. [39]), while it is not yet known when and how the reionization process had proceeded. If there are ionized electrons in the IGM, these electrons possibly scatter the CMB photons and cause damping in the angular power spectrum. The amount of the damping in the temperature fluctuations can be estimated as $\exp(-\tau)$, where τ is the optical depth of Thomson scattering defined as

$$\tau \equiv \int_{t_{\rm rec}}^{t_0} c{\rm d}t n_{\rm e} \sigma_{\rm T}. \tag{13}$$

In Fig. 6, the dependence of the angular power spectrum on the optical depth is shown. There exists an enhancement of the power spectrum for small ℓ for the model with $\tau = 0.5$ which is due to the Doppler effect caused by the peculiar motion of ionized regions.

3.6. *Miscellaneous*

The angular power spectrum obviously depends on the initial power law index $n_{\rm s}$. The dependence of $n_{\rm s}$ on the angular power spectrum can be approximately described as $C_\ell(n) \propto \ell^{n_{\rm s}-1} C_\ell(n=1)$

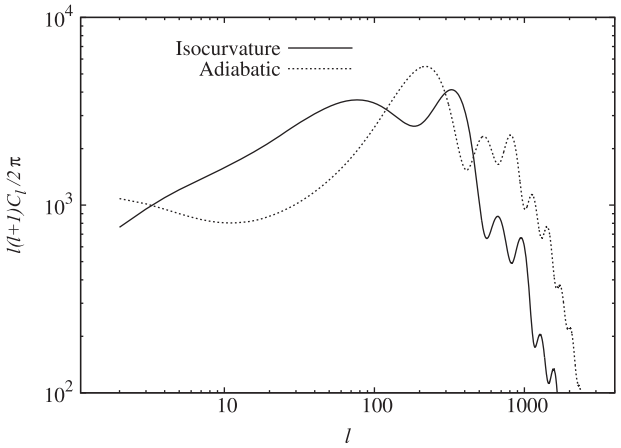

Fig. 5. The CMB angular power spectrum for isocurvature and adiabatic initial conditions. In order to make the peaks for the isocurvature case prominent, we adopt the scalar power law index $n_{\rm s} = 2$ instead of 1 for the adiabatic case.

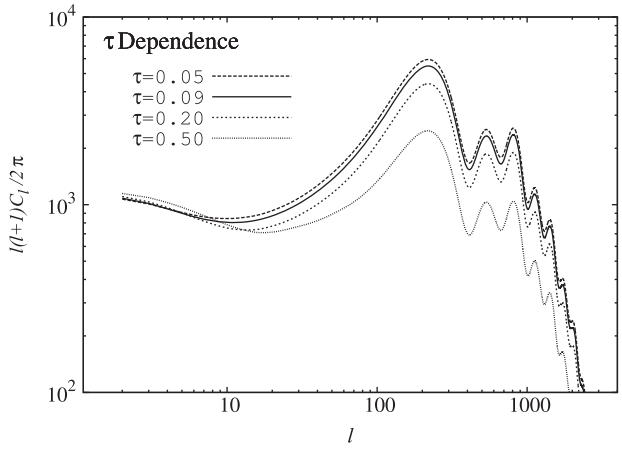

Fig. 6. Optical depth dependence on the CMB angular power spectrum.

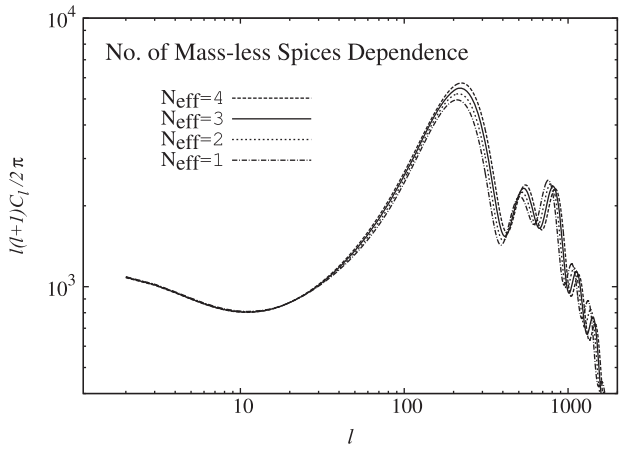

Fig. 7. The dependence of effective numbers of massless species on the CMB angular power spectrum.

for large ℓ (see Eq. (3.4) of Ref. [40]). There is degeneracy between the power law index and the optical depth since both larger n_s and lower τ increase the overall amplitude of the power spectrum on intermediate and small scales.

The dependence on the number of light species such as neutrinos shown in Fig. 7 can be understood as follows. If there exists an additional massless component, the matter–radiation equality shifts to the later epoch, which boosts the first peak height in the same manner as decreasing the matter density. Moreover, both the horizon size and the sound horizon size are reduced with an additional massless component, which shifts the peak locations to the high multipoles. This also enhances the diffusion damping scale. Finally, the anisotropic stress of neutrinos suppresses the small scale power. See, e.g., Ref. [41].

If there exist tensor perturbations, i.e., gravitational waves, they generate temperature anisotropies due to the Sachs–Wolfe effect on very large scales. Therefore, a certain fraction of tensor modes modify the shape and the amplitude of the angular power spectrum for very small ℓ, as shown in Fig 8. Here, we adopt the scalar–tensor ration $r = 0.2$ as inspired by the recent claim of B-mode polarization detection by BICEP2 [42].

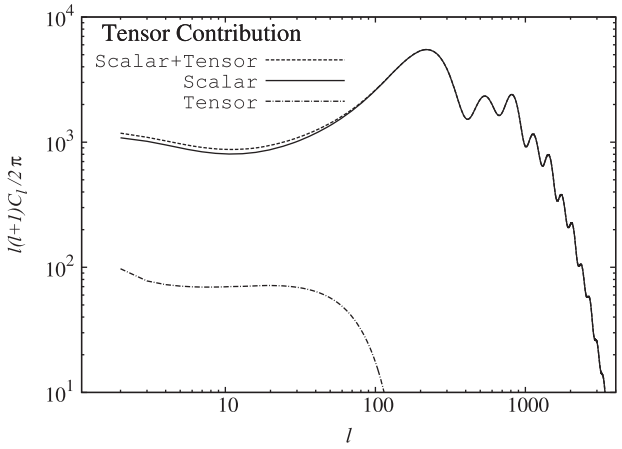

Fig. 8. Tensor contribution to the CMB angular power spectrum. Here we adopt the scalar–tensor ration to be 0.2.

4. To the future

In the last few decades, CMB has been the one of the most actively studied probes of cosmology. The angular power spectrum of temperature anisotropies is measured up to the third acoustic peaks by WMAP and $\ell \sim 2000$ by PLANCK, or at even finer angular scales by ground-based experiments such as ACT [43] and SPT [44]. Now the existence of diffusion damping is confirmed as well as acoustic oscillations and the Sachs–Wolfe plateau. To find non-Gaussisan statistics in the CMB temperature map, which could be a probe of the detailed mechanism of inflation, becomes the next major issue, while the recent PLANCK result sets stringent constraints on it [32].

The current hottest topic is the possible detection by BICEP2 of B-mode polarization induced by tensor perturbations [42]. Their reported value of the tensor–scalar ratio of the power spectrum $r = 0.2$ is, however, too large to be consistent with the PLANCK temperature observations unless, for example, a negative running spectral index is introduced. One cannot say anything conclusive until the PLANCK team announce their polarization results some time this year. Anyway, if it turns out that r is of the order of 0.1, we have a strong hope of measuring the spectral index of the tensor mode with high precision, which makes it possible to check the consistency relation of the single field slow roll inflation model with next-generation satellite experiments such as LiteBIRD, PIXIE, CoRE, and PRISM. This would provide stark evidence of the existence of inflation.

Observations of CMB can also be a probe of the thermal history of the universe. Overall heat generation in the early universe can be estimated by all-sky CMB spectrum distortions which have not been detected yet. PIXIE (Primordial Inflation Explorer) proposes to detect distortions as well as B-mode polarization of CMB. Other experiments to measure the CMB spectrum with high precision, such as DIMES and FIRAS II, are also proposed. Polarization also offers a unique probe of the reionization of the universe since polarization directly carries information of photons' last scatterings. Moreover, theory leads to the expected existence of a power spectrum on scales below diffusion dumping which is generated by peculiar motions of ionized bubbles at the epoch of reionization [45–47]. This additional spectrum will be detected by future experiments with much higher angular resolution than PLANCK. To eliminate contamination from other sources such as the Sunyaev–Zel'dovich effect from clusters of galaxies, or emissions from radio galaxies, measurements at multiple frequencies are essential. To study the reionization process in detail, a collaboration with the Square Kilometer Array (SKA), an international project using an enormous radio interferometer to find traces of neutral

hydrogen in the CMB through redshifted 21 cm signals, would be extremely fruitful. Construction of the SKA is scheduled to begin in 2016 for initial observations by 2019 and full operation by 2024.

In the next decade, I expect the CMB to become more and more important for studying astrophysical phenomena such as the Dark Ages and cosmic dawn, although CMB still keeps its current status as the best probe of cosmology.

Acknowledgments

N. S. is supported by Grant-in-Aid for Scientific Research No. 25287057 and would like to express gratitude to Hiroyuki Tashiro.

References

[1] A. A. Penzias and R. W. Wilson, ApJ, **142**, 419 (1965).
[2] R. A. Alpher and R. Herman, Nature, **162**, 774 (1948).
[3] R. K. Sachs and A. M. Wolfe, ApJ, **147**, 73 (1967).
[4] J. Silk, ApJ, **151**, 459 (1968).
[5] P. J. E. Peebles and J. T. Yu, ApJ, **162**, 815 (1970).
[6] Y. B. Zeldovich and R. A. Sunyaev, Astrophys. Space Sci., **4**, 301 (1969).
[7] R. A. Sunyaev and Y. B. Zeldovich, Astrophys. Space Sci., **7**, 3 (1970).
[8] R. A. Sunyaev and Y. B. Zeldovich, CoASP, **4**, 173 (1972).
[9] R. A. Sunyaev and I. B. Zeldovich, Annu. Rev. Astron. Astrophys., **18**, 537 (1980).
[10] E. M. Lifshitz and I. M. Khalatnikov, Adv. Phys., **12**, 185 (1963).
[11] A. D. Sakharov, JETP, **22**, 241 (1966).
[12] M. L. Wilson and J. Silk, ApJ, **243**, 14 (1981).
[13] M. L. Wilson, ApJ, **273**, 2 (1983).
[14] N. Vittorio and J. Silk, ApJL, **285**, L39 (1984).
[15] J. R. Bond and G. Efstathiou, ApJL, **285**, L45 (1984).
[16] J. R. Bond and G. Efstathiou, MNRAS, **226**, 655 (1987).
[17] J. M. Bardeen, Phys. Rev. D, **22**, 1882 (1980).
[18] H. Kodama and M. Sasaki, Prog. Theor. Phys. Supp., **78**, 1 (1984).
[19] N. Sugiyama, Prog. Theor. Phys., **81**, 1021 (1989).
[20] N. Sugiyama and N. Gouda, Prog. Theor. Phys., **88**, 803 (1992).
[21] G. F. Smoot, M. V. Gorenstein, and R. A. Muller, Phys. Rev. Lett., **39**, 898 (1977).
[22] G. F. Smoot and P. M. Lubin, ApJL, **234**, L83 (1979).
[23] E. S. Cheng, P. R. Saulson, D. T. Wilkinson, and B. E. Corey, ApJL, **232**, L139 (1979).
[24] J. C. Mather, E. S. Cheng, R. E. Eplee, Jr., R. B. Isaacman, S. S. Meyer, R. A. Shafer, R. Weiss, E. L. Wright, C. L. Bennett, N. W. Boggess, E. Dwek, S. Gulkis, M. G. Hauser, M. Janssen, T. Kelsall, P. M. Lubin, S. H. Moseley, Jr., T. L. Murdock, R. F. Silverberg, G. F. Smoot, and D. T. Wilkinson, ApJL, **354**, L37 (1990).
[25] J. C. Mather, E. S. Cheng, D. A. Cottingham, R. E. Eplee, Jr., D. J. Fixsen, T. Hewagama, R. B. Isaacman, K. A. Jensen, S. S. Meyer, P. D. Noerdlinger, S. M. Read, L. P. Rosen, R. A. Shafer, E. L. Wright, C. L. Bennett, N. W. Boggess, M. G. Hauser, T. Kelsall, S. H. Moseley, Jr., R. F. Silverberg, G. F. Smoot, R. Weiss, and D. T. Wilkinson, ApJ, **420**, 439 (1994).
[26] D. J. Fixsen, E. S. Cheng, J. M. Gales, J. C. Mather, R. A. Shafer, and E. L. Wright, ApJ, **473**, 576 (1996).
[27] G. F. Smoot, C. L. Bennett, A. Kogut, E. L. Wright, J. Aymon, N. W. Boggess, E. S. Cheng, G. de Amici, S. Gulkis, M. G. Hauser, G. Hinshaw, P. D. Jackson, M. Janssen, E. Kaita, T. Kelsall, P. Keegstra, C. Lineweaver, K. Loewenstein, P. Lubin, J. Mather, S. S. Meyer, S. H. Moseley, T. Murdock, L. Rokke, R. F. Silverberg, L. Tenorio, R. Weiss, and D. T. Wilkinson, ApJL, **396**, L1 (1992).
[28] W. Hu, N. Sugiyama, and J. Silk, Nature, **386**, 37 (1997).
[29] C. L. Bennett, M. Halpern, G. Hinshaw, N. Jarosik, A. Kogut, M. Limon, S. S. Meyer, L. Page, D. N. Spergel, G. S. Tucker, E. Wollack, E. L. Wright, C. Barnes, M. R. Greason, R. S. Hill, E. Komatsu, M. R. Nolta, N. Odegard, H. V. Peiris, L. Verde, and J. L. Weiland, ApJS, **148**, 1 (2003).

[30] D. N. Spergel, L. Verde, H. V. Peiris, E. Komatsu, M. R. Nolta, C. L. Bennett, M. Halpern, G. Hinshaw, N. Jarosik, A. Kogut, M. Limon, S. S. Meyer, L. Page, G. S. Tucker, J. L. Weiland, E. Wollack, and E. L. Wright, ApJS, **148**, 175 (2003).
[31] P. A. R. Ade et al. [Planck Collaboration], arXiv:1303.5062.
[32] P. A. R. Ade et al. [Planck Collaboration], arXiv:1303.5076.
[33] W. Hu and N. Sugiyama, Phys. Rev. D, **51**, 2599 (1995).
[34] M. White and W. Hu, Astron. Astrophys., **321**, 8 (1997).
[35] W. Hu and N. Sugiyama, Phys. Rev. D, **50**, 627 (1994).
[36] M. J. Rees and D. W. Sciama, Nature, **217**, 511 (1968).
[37] L. F. Abbott and R. K. Schaefer, ApJ, **308**, 546 (1986).
[38] S. Weinberg, *Cosmology*, (Oxford University Press, Oxford, 2008).
[39] X. Fan, M. A. Strauss, R. H. Becker, R. L. White, J. E. Gunn, G. R. Knapp, G. T. Richards, D. P. Schneider, J. Brinkmann, and M. Fukugita, AJ, **132**, 117 (2006).
[40] N. Sugiyama, ApJS, **100**, 281 (1995).
[41] G. Hinshaw, D. Larson, E. Komatsu, D. N. Spergel, C. L. Bennett, J. Dunkley, M. R. Nolta, M. Halpern, R. S. Hill, N. Odegard, L. Page, K. M. Smith, J. L. Weiland, B. Gold, N. Jarosik, A. Kogut, M. Limon, S. S. Meyer, G. S. Tucker, E. Wollack, and E. L. Wright, ApJS, **208**, 19 (2013).
[42] P. A. R. Ade et al. [BICEP2 Collaboration], arXiv:1403.3985.
[43] S. Das, T. Louis, M. R. Nolta, G. E. Addison, E. S. Battistelli, J. Bond, E. Calabrese, D. C. M. J. Devlin, S. Dicker, J. Dunkley, R. Dünner, J. W. Fowler, M. Gralla, A. Hajian, M. Halpern, M. Hasselfield, M. Hilton, A. D. Hincks, R. Hlozek, K. M. Huffenberger, J. P. Hughes, K. D. Irwin, A. Kosowsky, R. H. Lupton, T. A. Marriage, D. Marsden, F. Menanteau, K. Moodley, M. D. Niemack, L. A. Page, B. Partridge, E. D. Reese, B. L. Schmitt, N. Sehgal, B. D. Sherwin, J. L. Sievers, D. N. Spergel, S. T. Staggs, D. S. Swetz, E. R. Switzer, R. Thornton, H. Trac, and E. Wollack, arXiv:1301.1037.
[44] K. T. Story, C. L. Reichardt, Z. Hou, R. Keisler, K. A. Aird, B. A. Benson, L. E. Bleem, J. E. Carlstrom, C. L. Chang, H.-M. Cho, T. M. Crawford, A. T. Crites, T. de Haan, M. A. Dobbs, J. Dudley, B. Follin, E. M. George, N. W. Halverson, G. P. Holder, W. L. Holzapfel, S. Hoover, J. D. Hrubes, M. Joy, L. Knox, A. T. Lee, E. M. Leitch, M. Lueker, D. Luong-Van, J. J. McMahon, J. Mehl, S. S. Meyer, M. Millea, J. J. Mohr, T. E. Montroy, S. Padin, T. Plagge, C. Pryke, J. E. Ruhl, J. T. Sayre, K. K. Schaffer, L. Shaw, E. Shirokoff, H. G. Spieler, Z. Staniszewski, A. A. Stark, A. van Engelen, K. Vanderlinde, J. D. Vieira, R. Williamson, and O. Zahn, ApJ, **779**, 86 (2013).
[45] R. A. Sunyaev and I. B. Zeldovich, MNRAS, **190**, 413 (1980).
[46] A. Gruzinov and W. Hu, ApJ, **508**, 435 (1998).
[47] A. J. Benson, A. Nusser, N. Sugiyama, and C. G. Lacey, MNRAS, **320**, 153 (2001).